GSA Data Repository Item 2019163

Ming Lei, Jian-Lin Chen, Ji-Feng Xu, Yun-Chuan Zeng, and Qiu-Wei Xiong, 2019, Late Cretaceous magmatism in the NW Lhasa Terrane, southern Tibet: Implications for crustal thickening and initial surface uplift: GSA Bulletin, https://doi.org/10.1130/B31915.1.

Data Repository

TABLES

TABLE DR1: LA-ICP-MS zircon U-Pb data of GPs and XPs.

TABLE DR2: Late Cretaceous (~90 Ma) magmatic rocks within the NW Lhasa terrane.

FIGURES

FIGURE DR1: SiO_2 vs. P_2O_5 diagram for Xiongma granites.

FIGURE DR2: 1/Sr vs. $^{87}Sr/^{86}Sr_{(i)}$ diagram for Xiongma granites.

TEXTS

TEXT DR1: The calculation of initial whole rock Sr-Nd and zircon Hf isotopic ratios of GPs and XPs.

TEXT DR2: The calculation of the crustal thickness of the NW Lhasa terrane since the Cretaceous.

TABLE DR1. LA-ICP-MS zircon U-Pb data of GPs and XPs.

Spot	Th(ppm)	U(ppm)	Th/U	$^{207}Pb/^{206}Pb$	1σ	$^{207}Pb/^{235}U$	1σ	$^{206}Pb/^{238}U$	1σ	$^{207}Pb/^{235}U$(Ma)	1σ	$^{206}Pb/^{238}U$(Ma)	1σ	Conc.(%）
13GJ-07														
13GJ-07-03	167	198	0.8	0.05102	0.00511	0.08593	0.00750	0.01307	0.00025	84	7	84	2	99%
13GJ-07-14	238	231	1.0	0.04952	0.00404	0.08886	0.00685	0.01341	0.00026	86	6	86	2	99%
13GJ-07-20	181	184	1.0	0.05100	0.00548	0.08793	0.00912	0.01327	0.00028	86	9	85	2	99%
13GJ-07-17	188	177	1.1	0.04991	0.00524	0.08751	0.00906	0.01313	0.00029	85	8	84	2	98%
13GJ-07-18	137	158	0.9	0.04795	0.00569	0.08517	0.00992	0.01315	0.00030	83	9	84	2	98%
13GJ-07-21	163	144	1.1	0.05110	0.00697	0.08953	0.01165	0.01335	0.00036	87	11	85	2	98%
13GJ-07-02	434	306	1.4	0.05021	0.00396	0.08834	0.00662	0.01315	0.00021	86	6	84	1	97%
13GJ-07-16	109	164	0.7	0.05010	0.00584	0.08859	0.01019	0.01315	0.00027	86	10	84	2	97%
13GJ-07-11	173	195	0.9	0.05283	0.00534	0.09425	0.00932	0.01327	0.00025	91	9	85	2	92%
13GJ-08														
13GJ-08-03	253	238	1.1	0.04852	0.00416	0.08521	0.00705	0.01301	0.00021	83	7.	83	1	99%
13GJ-08-02	119	109	1.1	0.04929	0.00724	0.08684	0.01259	0.01334	0.00035	85	12	85	2	98%
13GJ-08-08	326	288	1.1	0.04880	0.00421	0.08674	0.00728	0.01336	0.00023	84	7	86	1	98%
13GJ-08-12	368	300	1.2	0.05072	0.00460	0.09014	0.00727	0.01330	0.00025	88	7	85	2	97%
13GJ-08-20	174	180	1.0	0.04843	0.00777	0.09019	0.01380	0.01337	0.00030	88	13	86	2	97%
13GJ-08-07	117	129	0.9	0.05241	0.00852	0.08933	0.01319	0.01314	0.00035	87	12	84	2	96%
13GJ-08-23	228	189	1.2	0.05112	0.00485	0.09144	0.00834	0.01336	0.00026	89	8	86	2	96%
13GJ-08-10	205	210	1.0	0.05119	0.00688	0.08825	0.01173	0.01283	0.00026	86	11	82	2	95%
13GJ-08-17	96	120	0.8	0.05149	0.00635	0.08918	0.01050	0.01296	0.00033	87	10	83	2	95%
13GJ-08-18	313	305	1.0	0.05093	0.00439	0.09285	0.00760	0.01339	0.00022	90	7	86	1	94%
13GJ-08-14	153	163	0.9	0.05375	0.00475	0.09789	0.00908	0.01328	0.00030	95	8	85	2	89%
13XM-05														
13XM-05-01	1094	1395	0.8	0.04810	0.00352	0.08998	0.00654	0.01356	0.00017	87.5	6.1	86.9	1.1	99%
13XM-05-02	804	1160	0.7	0.04972	0.00387	0.09346	0.00708	0.01366	0.00021	90.7	6.6	87.5	1.3	96%
13XM-05-04	888	1073	0.8	0.04830	0.00396	0.08873	0.00699	0.01355	0.00019	86.3	6.5	86.7	1.2	99%
13XM-05-05	1159	1435	0.8	0.04767	0.00371	0.08968	0.00679	0.01364	0.00019	87.2	6.3	87.4	1.2	99%
13XM-05-07	6235	2177	2.9	0.04950	0.00274	0.09526	0.00506	0.01390	0.00017	92.4	4.7	89.0	1.1	96%
13XM-05-08	1753	1807	1.0	0.04773	0.00281	0.08954	0.00523	0.01352	0.00017	87.1	4.9	86.6	1.1	99%

13XM-05-11	1198	1504	0.8	0.05006	0.00333	0.09198	0.00604	0.01340	0.00017	89.3	5.6	85.8	1.1	95%
13XM-05-12	1898	848	2.2	0.04980	0.00602	0.08875	0.01060	0.01336	0.00024	86.3	9.9	85.6	1.5	99%
13XM-05-15	1544	1744	0.9	0.05010	0.00290	0.09203	0.00530	0.01332	0.00016	89.4	4.9	85.3	1.0	95%
13XM-05-16	3228	2420	1.3	0.04817	0.00281	0.08928	0.00499	0.01357	0.00015	86.8	4.7	86.9	1.0	99%
13XM-05-17	877	1287	0.7	0.04850	0.00423	0.08869	0.00776	0.01336	0.00020	86.3	7.2	85.5	1.3	99%
13XM-05-18	661	1121	0.6	0.04821	0.00482	0.08718	0.00844	0.01313	0.00021	84.9	7.9	84.1	1.3	99%
13XM-05-19	303	533	0.6	0.04982	0.00756	0.09288	0.01375	0.01395	0.00026	90.2	12.8	89.3	1.7	99%
13XM-05-20	965	1544	0.6	0.04801	0.00367	0.08827	0.00652	0.01339	0.00018	85.9	6.1	85.7	1.1	99%
13XM-05-21	281	576	0.5	0.04858	0.00781	0.08713	0.01368	0.01331	0.00029	84.8	12.8	85.2	1.8	99%
13XM-05-22	1853	1747	1.1	0.05002	0.00395	0.08955	0.00648	0.01342	0.00018	87.1	6.0	85.9	1.2	98%
13XM-05-24	1080	1316	0.8	0.04966	0.00419	0.09157	0.00788	0.01326	0.00021	89.0	7.3	84.9	1.3	95%
13XM-10														
13XM-10-11	1381	1914	0.7	0.04845	0.00283	0.09412	0.00539	0.01414	0.00017	91.3	5.0	90.5	1.1	99%
13XM-10-06	2129	2078	1.0	0.04930	0.00305	0.09236	0.00561	0.01374	0.00019	89.7	5.2	88.0	1.2	98%
13XM-10-16	1464	1604	0.9	0.04900	0.00323	0.09199	0.00586	0.01375	0.00016	89.4	5.5	88.1	1.0	98%
13XM-10-20	2112	2139	1.0	0.04898	0.00324	0.09237	0.00605	0.01376	0.00017	89.7	5.6	88.1	1.1	98%
13XM-10-01	1704	1801	0.9	0.04922	0.00289	0.09368	0.00538	0.01382	0.00019	90.9	5.0	88.5	1.2	97%
13XM-10-05	724	1176	0.6	0.04936	0.00461	0.09289	0.00873	0.01378	0.00022	90.2	8.1	88.2	1.4	97%
13XM-10-18	1027	1492	0.7	0.04927	0.00318	0.09301	0.00599	0.01377	0.00018	90.3	5.6	88.2	1.1	97%
13XM-10-21	1063	1310	0.8	0.05060	0.00380	0.09306	0.00646	0.01376	0.00020	90.4	6.0	88.1	1.3	97%
13XM-10-09	785	1165	0.7	0.04524	0.00358	0.08788	0.00706	0.01381	0.00021	85.5	6.6	88.4	1.3	96%
13XM-10-14	792	1247	0.6	0.05101	0.00388	0.09450	0.00722	0.01382	0.00018	91.7	6.7	88.5	1.2	96%
13XM-10-17	1160	1415	0.8	0.04649	0.00328	0.08775	0.00606	0.01387	0.00019	85.4	5.7	88.8	1.2	96%
13XM-10-03	1033	1638	0.6	0.05096	0.00325	0.09463	0.00584	0.01373	0.00018	91.8	5.4	87.9	1.2	95%
13XM-10-12	1108	1485	0.7	0.04578	0.00282	0.08750	0.00530	0.01390	0.00017	85.2	4.9	89.0	1.1	95%
13XM-10-15	1128	1729	0.7	0.05097	0.00301	0.09613	0.00548	0.01389	0.00020	93.2	5.1	88.9	1.3	95%
13XM-10-22	1226	1489	0.8	0.04460	0.00380	0.08435	0.00712	0.01374	0.00018	82.2	6.7	88.0	1.1	93%
13XM-10-08	1134	1463	0.8	0.05283	0.00383	0.09841	0.00683	0.01385	0.00021	95.3	6.3	88.7	1.3	92%
13XM-10-13	943	1412	0.7	0.05217	0.00413	0.09894	0.00781	0.01378	0.00017	95.8	7.2	88.2	1.1	91%
13XM-10-24	955	1183	0.8	0.05289	0.00401	0.10036	0.00761	0.01398	0.00020	97.1	7.0	89.5	1.2	91%
13XM-10-04	1706	1832	0.9	0.05322	0.00378	0.09814	0.00674	0.01350	0.00017	95.1	6.2	86.5	1.1	90%
13XM-10-07	1169	1395	0.8	0.04305	0.00365	0.08013	0.00676	0.01342	0.00020	78.3	6.4	86.0	1.3	90%

13XM-12														
13XM-12-23	1303	3203	0.4	0.0481	0.0020	0.0913	0.0038	0.0138	0.0002	88.7	3.5	88.2	1.2	99%
13XM-12-7	3892	1358	2.9	0.0466	0.0031	0.0873	0.0059	0.0135	0.0002	85.0	5.5	86.4	1.4	98%
13XM-12-9	10383	5561	1.9	0.0479	0.0014	0.0939	0.0027	0.0141	0.0002	91.1	2.5	90.2	1.1	98%
13XM-12-1	6837	3606	1.9	0.0495	0.0015	0.0954	0.0030	0.0139	0.0002	92.6	2.8	89.0	1.0	96%
13XM-12-5	11946	5108	2.3	0.0517	0.0030	0.0963	0.0027	0.0140	0.0002	93.3	2.5	89.3	1.1	95%
13XM-12-6	848	1511	0.6	0.0508	0.0026	0.0949	0.0045	0.0136	0.0002	92.1	4.2	87.2	1.0	94%
13XM-12-11	13637	5602	2.4	0.0505	0.0014	0.0973	0.0029	0.0137	0.0002	94.2	2.7	87.9	1.1	93%
13XM-12-8	1753	1140	1.5	0.0530	0.0046	0.0970	0.0074	0.0138	0.0003	94.0	6.8	88.1	1.6	93%
13XM-12-17	1722	1730	1.0	0.0516	0.0025	0.0989	0.0050	0.0139	0.0002	95.7	4.6	89.2	1.5	92%
13XM-12-13	1266	1990	0.6	0.0588	0.0082	0.0990	0.0057	0.0137	0.0003	95.9	5.2	88.0	1.6	91%
13XM-12-19	4102	3253	1.3	0.0558	0.0028	0.1054	0.0047	0.0140	0.0002	102	4.0	89.7	1.5	87%
13XM-12-3	7458	3611	2.1	0.0539	0.0017	0.1044	0.0035	0.0139	0.0001	101	3.0	88.7	0.9	87%

Note: Samples of 13XM-12 are MME and other samples of XPs are granites.

TABLE DR2. Late Cretaceous (~90 Ma) magmatic rocks within the NW Lhasa terrane.

Location	Type of rocks	Ages (Ma)	References
Zhuogapu	Basaltic andesite, Andesite, Dacite	91	Wang et al., 2014
Adang	Basalt, Andesite	91	Ma and Yue, 2010
Zhongcang	Granodiorite porphyry	88	Yu et al., 2011; Chen etal., 2015
Rutog	Granitic pluton, Granodiorite, Monzogranite	84-80	Zhao et al., 2008; Liu et al., 2016
Gaerqiong	Quartz diorite, Granodiorite	87	Lv et al., 2012; Yao et al., 2012
Coqen	Granite, Diabase	88	Qu et al., 2006; Xin et al., 2007
Azhang	Dacite	90	Sun et al., 2015
Amdo	Andesite	80	Chen et al., 2017b
Abushan	Andesite	75-79	Li et al., 2013
Baingoin	Dacite	92-94	Yi et al., 2018
Xiongba	abundant 90 Ma zircon xenocrysts of ultra-K volcanic rocks	90	Liu et al., 2013
Gaerqiong	Diorite porphhies	85	this study
Coqen	Granite, MMEs	88	this study

REFERENCES

Chen, J.L., Xu, J.F., Yu, H.X., Wang, B.D., Wu, J.B., and Feng, Y.X., 2015, Early late Cretaceous high-Mg# granitoids in southern Tibet: Implications for the early crustal thickening and tectonic evolution of the Tibetan Plateau: Lithos, v. 232, p. 12–22, doi:10.1016/j.lithos.2015.06.020.

Chen, S.S., Fan, W.M., Shi, R.D., Gong, X.H., and Wu, K., 2017b, Removal of deep lithosphere in ancient continental collisional orogens: A case study from central Tibet, China: Geochemistry. Geophysics. Geosystems, v. 18, p. 1225–1243, doi:10.1002/2016GC006678.

Li, Y.L., He, J., Wang, C.S., Santosh, M., Dai, J.G., Zhang, Y.X., Wei, Y.S., and Wang, J.G., 2013. Late Cretaceous K-rich magmatism in central Tibet: evidence for early elevation of the Tibetan plateau? : Lithos, v. 160, p. 1–13 ,doi:10.1016/j.lithos.2012.11.019.

Liu, D., Zhao, Z.D., Zhu, D.C., Niu, Y.L., and Harrison, T.M., 2013, Zircon xenocrysts in Tibetan ultrapotassic magmas: Imaging the deep crust through time: Geology, v. 42, p. 43–46, doi: 10.1130/G34902.1.

Liu, H., Wang., B.D., Chen, L., Li X.B., and Wang, L.Q., 2015, Zircon U-Pb geochronology, geochemistry and its tectonic significance of the Rutog granitic batholith in the Northwest Lhasa Terrane [in Chinese with English abstract]: Geotectonica et Metallogenia, v. 39, p. 1141–1155.

Lv, L.N. 2012, Metallogenic model of rich iron and copper (gold) deposit in western part of Bangong Co-Nujiang metallogenic belt, Tibet [Master's Degree dissertation], Chinese Academy of Geological Sciences, Beijing [in Chinese with English abstract].

Ma, G.L., and Yue, Y.H., 2010, Cretaceous volcanic rocks in northern Lhasa Block: constraints on the tectonic evolution of the Gangdese Arc [in Chinese with English abstract]: Acta Petrolei Et Mineralogica, v. 29, p. 525–538.

Qu, X.M., Xin, H.B., Xu, W.Y., Yang, Z.S., and Li, Z.Q., 2006, Discovery and singificane of copperbearing bimodal rocks series in Coqin area of Tibet [in Chinese with an English abstract]: Acta Petrolei Sinica, v. 22, p. 707–716.

Sun, G.Y., Hu, X.M., Zhu, D.C., Hong, W.T., Wang, J.G., and Wang, Q., 2015b, Thickened juvenile lower crust-derived ~90 Ma adakitic rocks in the central Lhasa terrane, Tibet: Lithos, v. 224: p. 225–239, doi:10.1016/j.lithos.2015.03.010.

Wang, Q., Zhu, D.C., Zhao, Z.D., Liu, S.A., Chung, S.L., Li, S.M., Liu, D., Dai, J.G., Wang, L.Q., and Mo, X.X., 2014, Origin of the ca. 90 Ma magnesia-rich volcanic rocks in SW Nyima, central Tibet: Products of lithospheric delamination beneath the Lhasa-Qiangtang collision zone: Lithos, v. 198–199, p. 24–37, doi:10.1016 /j .lithos.2014 .03 .019.

Xin, H.B., Qu, X.M., Ren, L.K., and Zhang, L.Y., 2007, The material source and genesis of copper-bearing bimodal rocks series in Coqin County, Western Tibet [in Chinese with English abstract]: Acta Geologica Sinica, v. 81, p. 939–935.

Yao, X.F., Tang, J.X., Li, Z.J., Deng, S.L., Ding, S.H., Zheng, H., and Zhang, Z., 2012, Magma origin of two plutons from gaerqiong copper-gold deposit and it's geological significance, western Bangonghu-Nujiang metallogenic belt, Tibet implication from Hf isotope characteristics [in Chinese with English abstract]: Journal of Jilin University, v. 42, p. 188–197.

Yi, J.K., Wang, Q., Zhu, D.C., Li, S.M., Liu, S.A., Wang, R., Zhang, L.L., and Zhao, Z.D., 2018, Westward-Younging high-Mg adakitic magmatism in Central Tibet: Record of a westward-Migrating lithospheric foundering beneath the Lhasa-Qiangtang collision zone during the late Cretaceous: Lithos, v.316–317, p. 92–103, doi:10.1016/j.lithos.2018.07.001.

Yu, H.X., Chen, J.L., Xu, J.F., Wang, B.D., Wu, J.B., and Liang, Y.H., 2011, Geochemistry and origin of Late Cretaceous (~90 Ma) mineral porphyry of Balazha in mid-northern Lhasa terrane, Tibet [in Chinese with English abstract]: Acta Petrolei Sinica, v. 27, p. 2011–2022.

Zhao, T.P., Zhou, M.F., Zhao, J.H., Zhang, K.J., and Chen, W., 2008, Geochronology and geochemistry of the ca.80 Ma Rutog granitic pluton, northwestern Tibet: implications for the tectonic evolution of the Lhasa Terrane: Geological Magazine, v. 145, p. 845–857, doi: 10.1017/S0016756808005025.

FIG. DR1. SiO_2 vs. P_2O_5 diagram for Xiongma granites.

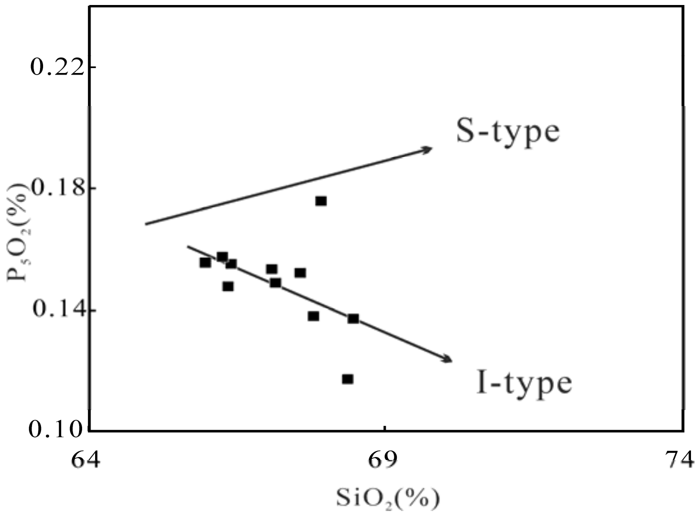

FIG. DR2. 1/Sr vs. $^{87}Sr/^{86}Sr_{(i)}$ diagram for Xiongma granites.

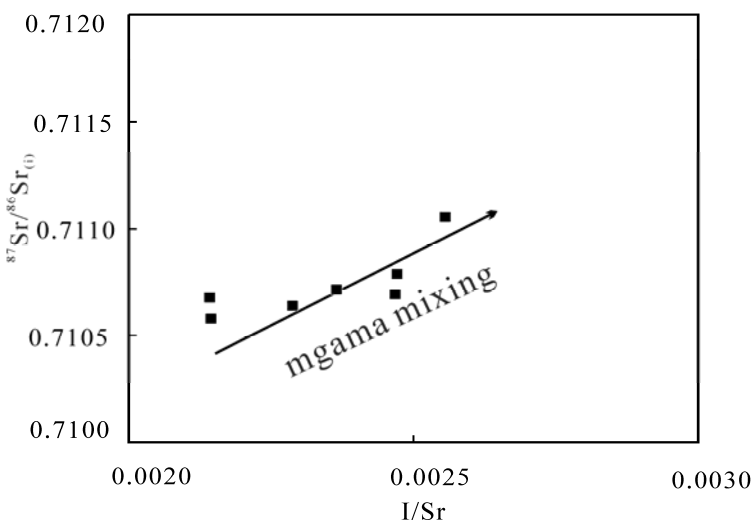

TEXT DR1. The calculation of initial whole rock Sr-Nd and zircon Hf isotopic ratios of GPs and XPs.

$(^{87}Sr/^{86}Sr)_i = (^{87}Sr/^{86}Sr)_m - (^{87}Rb/^{86}Sr) \times (e^{\lambda T} - 1)$;

$(^{143}Nd/^{144}Nd)_t = (^{143}Nd/^{144}Nd)_m - (^{147}Sm/^{144}Nd) \times (e^{\lambda T} - 1)$;

$\varepsilon_{Nd(t)} = [(^{143}Nd/^{144}Nd)s/(^{143}Nd/^{144}Nd)_{CHUR} - 1] \times 10{,}000$ (DePaolo, 1988) ;

In the calculation, $(^{143}Nd/^{144}Nd)_{CHUR}=0.512638$, $(^{147}Sm/^{144}Nd)_{CHUR}=0.1967$, $\lambda_{Rb}=1.42\times10^{-11}$/year (Steiger and Jager, 1977), $\lambda_{Sm} = 6.54 \times 10^{-12}$/ year (Lugmair and Marti, 1978), and t= crystallization time of samples.

$\varepsilon Hf_{(t)} = [^{176}Hf/^{177}Hf_Z / {}^{176}Hf/^{177}Hf_{CHUR(T)} - 1] \times 10{,}000$;

$^{176}Hf/^{177}Hf_{CHUR(T)} = {}^{176}Hf/^{177}Hf_{CHUR(0)} - {}^{176}Lu/^{177}Hf_{CHUR} \times (e^{\lambda T} - 1)$;

$T_{DM} = (1 / \lambda) \times \ln[1+(^{176}Hf/^{177}Hf_{DM} - {}^{176}Hf/^{177}Hf_Z)/(^{176}Lu/^{177}Hf_{DM} - {}^{176}Lu/^{177}Hf_Z)]$;

$T_{DM}^{C} = T_{DM} - (T_{DM} - T) \times [(f_C^{C} - f_Z) / (f_C^{C} - f_{DM})]$;

$f_{Lu/Hf} = {}^{176}Hf/^{177}Hf_Z / {}^{176}Lu/^{177}Hf_{CHUR} - 1$,

where f_{CC}, f_Z and f_{DM} are the $f_{Lu/Hf}$ values of the continental crust, zircon sample and the depleted mantle; subscript Z = analyzed zircon sample, CHUR = chondritic uniform reservoir; DM = depleted mantle; t = crystallization time of zircon; $\lambda = 1.867\times10^{-11}$ year^{-1}, decay constant of ^{176}Lu (Soderlund et al., 2004); $^{176}Hf/^{177}Hf_{DM} = 0.28325$ (Nowell et al., 1998); $^{176}Lu/^{177}Hf_{DM} = 0.0384$ (Griffin et al., 2000); present-day $^{176}Hf/^{177}Hf_{CHUR(0)} = 0.282785$; $^{176}Hf/^{177}Hf_{CHUR} = 0.0336$ (Bouvier et al., 2008); $^{176}Hf/^{177}Hf_C^{C} = 0.015$.

REFERENCES

Bouvier, A., Vervoort ,J. D., and Patchett., P. J., 2008, The Lu–Hf and Sm–Nd isotopic composition of CHUR: constraints from unequilibrated chondrites and implications for the bulk composition of terrestrial planets: Earth and Planetary Science Letters, v.273, p. 48-57, doi:10.1016/j.epsl.2008.06.010.

DePaolo, D., J. 1988, Neodymium isotope geochemistry: an introduction, Springer-Verlag Berlin.

Griffin, W.L., Pearson, N.J., Belousova, E., Jackson, S.E., van Achterbergh, E., O'Reilly, S.Y., and Shee, S.R., 2000, The Hf isotope composition of cratonic mantle: LAM-MC-ICPMS analysis of zircon megacrysts in kimberlites: Geochim. Cosmochim. Acta, v. 64, p.133–147, doi:10.1016/S0016-7037(99)00343-9.

Lugmair, G.W., and Marti, K., 1978, Lunar initial 143Nd/144Nd: differential evolution of the lunar crust and mantle: Earth and Planetary Science Letters, v. 39, p. 349-357, doi:10.1016/0012-821X(78)90021-3.

Nowell, G.M., Kempton, P.D., Noble, S.R., Fitton, J.G., Saunders, A.D., Mahoney, J.J., and Taylor, R.N., 1998, High precision Hf isotope measurements of MORB and OIB by thermal ionisation mass spectrometry: insights into the depleted mantle: Chemical Geology, v. 149, p. 211–233, doi:10.1016/S0009-2541(98)00036-9.

Steiger, R., and Jäger, E., 1977, Subcommission on geochronology: convention on the use of decay constants in geochronology and cosmochronology: Earth and Planetary Science Letters, v. 36, p. 359–362, doi:10.1016/0012-821X(77)90060-7.

Söderlund, U., Patchett, P.J., Vervoort, J.D., and Isachsen, C.E., 2004, The ^{176}Lu decay constant determined by Lu–Hf and U–Pb isotope systematics of Precambrian mafic intrusions: Earth and Planetary Science Letters, v. 219, p. 311–324, doi:10.1016/S0012-821X(04)00012-3.

TEXT DR2. The calculation of crustal thickness of the NW Lhasa terrane since the Cretaceous.

The La/Yb and Sr/Y ratios of intermediate-silicic rocks for constructing correlation between and Moho depth is based on that the La/Yb and Sr/Y ratios of intermediate-silicic rocks can reflect intrinsically the presence of mineral assemblages (amphibole + plagioclase ± garnet) in the magma source region (Chapman et al., 2015; Profeta et al., 2015). Recently, the study of Hu et al. (2017) compiled the major and trace element data on Miocene and younger intrusive and extrusive rocks from six continental collisional orogens (including the Southern Tibet) and established the empirical relationships between geochemical indices and crustal thickness or Moho depth ($(La/Yb)_N = 2.94e^{(0.036D_M)}$, or $D_M = 27.78\ln[0.34(La/Yb)_N]$, where $(La/Yb)_N$ is whole rock value, and D_M is crustal thickness or Moho depth) by performing a least-squares regression through these data subsets. The empirical relationship of the La/Yb ratios of global intermediate rocks with crustal thickness defined by Hu et al. (2017) is used to track the crustal thickness of the NW Lhasa terrane since Cretaceous. The calculated results are listed below.

Sample	SB01-2	08YR11	DG05-1	NQ12-10	NQ09-1	SZ01-1*	SZ07-1	SZ10-1	GRC02-1	GRC03-2	DX2-1	DX13-1	NX5-2
E/L Cretaceous	E	E	E	E	E	E	E	E	E	E	E	E	E
Reference	1	1	1	1	1	1	1	1	1	1	1	1	1
Ages (Ma)	118.4	134.3	114.3	110.8	110.7	116.7	110.9	112.1	114.0	113.8	130.0	121.0	109.0
SiO_2 (wt. %)	71.7	63.6	67.1	59.5	69.3	64.8	63.5	64.5	64.6	65.3	66.5	68.1	67.5
La/Yb	11.4	11.6	7.6	14.4	15.0	12.2	10.8	12.5	14.2	15.7	8.1	9.1	13.0
Dm (Km)	26.9	27.4	15.7	33.4	34.6	28.8	25.4	29.5	33.0	35.8	17.5	20.7	30.6
Std (Km)	4.5	4.6	3.3	5.3	5.4	4.7	4.3	4.8	5.2	5.6	3.5	3.8	4.9
Sample	GB-8	DX2-1	DX13-1	NX5-2	GB-8	SZ48	DX19-1	DX19-3	CR-14	CR-15	CR-16	CR-24	CR-28
E/L Cretaceous	E	E	E	E	E	E	E	E	L	L	L	L	L
Reference	1	2	2	2	2	2	3	3	4	4	4	4	4
Ages (Ma)	116.0	130.0	121.3	108.4	116.3	111.0	108.0	108.0	88.0	88.0	88.0	88.0	88.0
SiO_2 (wt.%)	68.4	66.5	68.1	67.5	68.4	60.5	71.0	70.7	67.2	70.2	71.4	69.0	68.1
La/Yb	14.1	8.1	9.1	13.0	14.0	9.8	12.3	10.8	20.6	23.6	19.6	21.2	20.0
Dm (Km)	32.9	17.5	20.7	30.6	32.7	22.7	29.1	25.4	43.4	47.2	42.0	44.2	42.6
Std (Km)	5.2	3.5	3.8	4.9	5.2	4.0	4.7	4.3	6.5	7.0	6.3	6.6	6.4

Sample	CR-31	09ZC-09	09ZC-40	09ZC-41	09ZC-45	09ZC-46	09ZC-21	09ZC-22	09ZC-23	LS-74	LS-75	LS-H	LS-I
E/L Cretaceous	L	L	L	L	L	L	L	L	L	L	L	L	L
Reference	4	5	5	5	5	5	5	5	5	6	6	6	6
Ages (Ma)	88	88	88	88	88	88	88	88	88	90	90	90	90
SiO_2 (wt. %)	67.4	69.9	71.2	70.6	66.1		68.6	67.8	69.2	63.5	64.2	65.1	64.2
La/Yb	34.2	28.4	28.5	42.1	22.2	16.1	31.6	27.9	24	29.6	29.3	30.9	31.4
Dm (Km)	57.5	52.3	52.4	63.2	45.5	36.5	55.3	51.8	47.6	53.5	53.2	54.6	55.1
Std (Km)	8.4	7.7	7.7	9.1	6.8	5.7	8.1	7.6	7.1	7.8	7.8	8	8

Sample	LS-J	LS-K	LS-N	LS-O	LS-P	LS-Q	RT-1	RT-2-1	RT-2-2	RT-3-1	RT-4-1	RT-4-2	RT-4-3
E/L Cretaceous	L	L	L	L	L	L	L	L	L	L	L	L	L
Reference	6	6	6	6	6	6	7	7	7	7	7	7	7
Ages (Ma)	90	90	90	90	90	90	84	84	84	84	84	84	84
SiO_2 (wt. %)	66	63.3	64.4	63.9	64.6	65.4	65.7	67.8	68.4	69.5	69.6	70.1	71.3
La/Yb	30.6	29.6	30.1	30.2	29.5	29.9	28.6	29.4	28.4	36.5	32.7	29.5	35.1
Dm (Km)	54.4	53.5	53.9	54	53.4	53.7	52.5	53.3	52.3	59.3	56.2	53.4	58.2
Std (Km)	8	7.8	7.9	7.9	7.8	7.9	7.7	7.8	7.7	8.6	8.2	7.8	8.5

Sample	RT-5-1	RT-6-1	RT-7	RT-8	RT-9-1	RT-10-1	RT-10-2	RT-11	10RT-16	11BG01-1	13BG05-1	13BG05-2	13BG05-5
E/L Cretaceous	L	L	L	L	L	L	L	L	L	L	L	L	L
Reference	7	7	7	7	7	7	7	7	7	8	8	8	8
Ages (Ma)	84	84	84	84	84	84	84	84	84	93	93	93	93
SiO_2 (wt. %)	70.6	68.5	67.9	72.1	69.5	68	61.7	63.4	65.1	64.1	64.8	66.0	64.6
La/Yb	31.6	29.9	27.1	25.5	32.2	27.6	21	28.2	24.3	27.9	29.8	30.8	28.8
Dm (Km)	55.3	53.7	51	49.3	55.8	51.5	43.9	52.1	48	51.8	53.7	54.5	52.7
Std (Km)	8.1	7.9	7.5	7.3	8.1	7.6	6.6	7.7	7.1	7.6	7.9	8.0	7.7

Sample	13BG05-6	13BG05-7	13BG05-8	13BG05-9	13BG05-10	13XM-01	13XM-02	13XM-03	13XM-04	13XM-05	13XM-06	13XM-07	13XM-08
E/L Cretaceous	L	L	L	L	L	L	L	L	L	L	L	L	L
Reference	8	8	8	8	8	9	9	9	9	9	9	9	9
Ages (Ma)	93	93	93	93	93	88	88	88	88	88	88	88	88
SiO_2 (wt. %)	64.5	64.7	65.9	64.6	65.1	66.4	67.9	66.3	66	67.8	68.4	67.6	68.3
La/Yb	31.1	29.5	29.8	27.8	28.9	20.1	21	21.4	17	16	19	18.2	24
Dm (Km)	54.8	53.3	53.7	51.7	52.8	42.7	43.9	44.4	38	36.4	41.1	39.9	47.6
Std (Km)	8.0	7.8	7.9	7.6	7.7	6.4	6.6	6.7	5.8	5.6	6.2	6.1	7.1

Sample	13XM-10	13XM-11	13GJ-7	13GJ-8	13GJ-9	13GJ-10	13GJ-11	13GJ-12
E/L Cretaceous	L	L	L	L	L	L	L	L
Reference	9	9	9	9	9	9	9	9
Ages (Ma)	88	88	85	85	85	85	85	85
SiO_2 (wt. %)	67.1	67.1	60.6	59.5	62.4	63	62.7	61.2
La/Yb	16.2	21.6	24.5	19.7	22.4	21.3	26.7	23.4
Dm (Km)	36.7	44.7	48.2	42.1	45.7	44.3	50.6	46.9
Std (Km)	5.7	6.7	7.1	6.4	6.8	6.6	7.5	7

Note: std represents standard deviation, E represents the Early Cretaceous (140-110 Ma) intermediate-silicic rocks, and L represents the Late Cretaceous (~90 Ma) intermediate-silicic rocks rocks. D_M is crustal thickness or Moho depth. The data collected here are from: reference 1 (Zhu et al., 2011); reference 2 (Zhu et al., 2009); reference 3 (Zhou et al., 2008); reference 4 (Qu et al., 2006; Xin et al., 2007); references 5 (Yu et al., 2011; Chen et al., 2015); reference 6 (Sun et al., 2015b); references 7 (Zhao et al., 2008; Liu et al., 2016); reference 8 (Yi et al., 2018); and reference 9 (this study). It should be noted that samples which have high SiO_2 (>72 wt. %) or the significant mantle materials input are excluded from our analysis because their high values of La/Y may be the result of the magma evolution and cannot reflect their source character (Chapman et al., 2015).

REFERENCES

Chapman, J.B., Ducea, M.N., DeCelles, P. G., and Profeta, L., 2015, Tracking changes in crustal thickness during orogenic evolution with Sr/Y: An example from the North American Cordillera; Geology, v. 43, p. 919–922, doi: 10.1130/G36996.1.

Chen, J.L., Xu, J.F., Yu, H.X., Wang, B.D., Wu, J.B., and Feng, Y.X., 2015, Early late Cretaceous high-Mg# granitoids in southern Tibet: Implications for the early crustal thickening and tectonic evolution of the Tibetan Plateau: Lithos, v. 232, p. 12–22, doi:10.1016/j.lithos.2015.06.020.

Liu, H., Wang., B.D., Chen, L., Li X.B., and Wang, L.Q., 2015, Zircon U-Pb geochronology, geochemistry and its tectonic significance of the Rutog granitic batholith in the Northwest Lhasa Terrane [in Chinese with English abstract]: Geotectonica et Metallogenia, v. 39, p. 1141–1155.

Ma, G.L., and Yue, Y.H., 2010, Cretaceous volcanic rocks in northern Lhasa Block: constraints on the tectonic evolution of the Gangdese Arc [in Chinese with English abstract]: Acta Petrolei Et Mineralogica, v. 29, p. 525–538.

Profeta, L., Ducea, M.N., Chapman, J.B., Paterson, S.R., Gonzales, S.M., Kirsch, M., Petrescu, L., and DeCelles, P.G., 2015, Quantifying crustal thickness over time in magmatic arcs: Scientific Reports, v. 5, p. 17786, doi: 10.1038/srep17786.

Qu, X.M., Xin, H.B., Xu, W.Y., Yang, Z.S., and Li, Z.Q., 2006, Discovery and singificane of copperbearing bimodal rocks series in Coqin area of Tibet [in Chinese with an English abstract]: Acta Petrolei Sinica, v. 22, p. 707–716.

Sun, G.Y., Hu, X.M., Zhu, D.C., Hong, W.T., Wang, J.G., and Wang, Q., 2015b, Thickened juvenile lower crust-derived ~90 Ma adakitic rocks in the central Lhasa terrane, Tibet: Lithos, v. 224: p. 225–239, doi:10.1016/j.lithos.2015.03.010.

Wang, Q., Zhu, D.C., Zhao, Z.D., Liu, S.A., Chung, S.L., Li, S.M., Liu, D., Dai, J.G., Wang, L.Q., and Mo, X.X., 2014, Origin of the ca. 90 Ma magnesia-rich volcanic rocks in SW Nyima, central Tibet: Products of lithospheric delamination beneath the Lhasa-Qiangtang collision zone: Lithos, v. 198–199, p. 24–37, doi:10.1016 /j .lithos.2014 .03 .019.

Xin, H.B., Qu, X.M., Ren, L.K., and Zhang, L.Y., 2007, The material source and genesis of copper-bearing bimodal rocks series in Coqin County, Western Tibet [in Chinese with English abstract]: Acta Geologica Sinica, v. 81, p. 939–935.

Yi, J.K., Wang, Q., Zhu, D.C., Li, S.M., Liu, S.A., Wang, R., Zhang, L.L., and Zhao, Z.D., 2018, Westward-Younging high-Mg adakitic magmatism in Central Tibet: Record of a westward-Migrating lithospheric foundering beneath the Lhasa-Qiangtang collision zone during the late Cretaceous: Lithos, v.316–317, p. 92–103, doi:10.1016/j.lithos.2018.07.001.

Yu, H.X., Chen, J.L., Xu, J.F., Wang, B.D., Wu, J.B., and Liang, Y.H., 2011, Geochemistry and origin of Late Cretaceous (~90 Ma) mineral porphyry of Balazha in mid-northern Lhasa terrane, Tibet [in Chinese with English abstract]: Acta Petrolei Sinica, v. 27, p. 2011–2022.

Zhao, T.P., Zhou, M.F., Zhao, J.H., Zhang, K.J., and Chen, W., 2008, Geochronology and geochemistry of the ca.80 Ma Rutog granitic pluton, northwestern Tibet: implications for the tectonic evolution of the Lhasa Terrane: Geological Magazine, v. 145, p. 845–857, doi: 10.1017/S0016756808005025.

Zhou, C.Y., Zhu, D.C., Zhao, Z.D., Xu, J.F., Wang, L.Q., Chen, H.H., Xie, L.W., Dong, G.C., and Zhou, S., 2008, Petrogenesis of Daxiong pluton in western Gangdese, Tibet: zircon U-Pb dating and Hf isotopic constraints [in Chinese with English abstract]: Acta Petrolei Sinica, v. 24, p. 348–358.

Zhu, D.C., Mo, X.X., Niu, Y.L., Zhao, Z.D., Wang, L.Q., Liu, Y.S., and Wu, F.Y., 2009, Geochemical investigation of Early Cretaceous igneous rocks along an eastwest traverse throughout the central Lhasa Terrane, Tibet: Chemical Geology, v. 268, p. 298–312, doi: 10.1016 /j .chemgeo.2009.09.008.

Zhu, D.C., Zhao, Z.D., Niu, Y.L., Mo, X.X., Chung, S.L., Hou, Z.Q., Wang, L.Q., and Wu, F.Y., 2011, The Lhasa Terrane: Record of a microcontinent and its histories of drift and growth: Earth and Planetary Science Letters, v. 301, p. 241–255, doi:10.1016 /j .epsl.2010.11.005.